Vortex density fluctuations in quantum turbulence

A. W. Baggaley* and C. F. Barenghi
School of Mathematics and Statistics, University of Newcastle, Newcastle upon Tyne, NE1 7RU, UK

Turbulence in the low temperature phase of liquid helium is a complex state in which a viscous normal fluid interacts with an inviscid superfluid. In the former vorticity consists of eddies of all sizes and strengths; in the latter vorticity is constrained to quantized vortex lines. We compute the frequency spectrum of superfluid vortex density fluctuations and obtain the same $f^{-5/3}$ scaling which has been recently observed. We show that the scaling can be interpreted in terms of the spectrum of reconnecting material lines. To perform this calculation we have developed a vortex tree algorithm which considerably speeds up the evaluation of Biot-Savart integrals.

PACS numbers: 67.25.dk Vortices and turbulence in superfluid ^{4}He
47.32.C- Vortex dynamics
47.27.Gs Homogeneous isotropic turbulence

* a.w.baggaley@ncl.ac.uk

Current theoretical and experimental work explores the relation between turbulence in an ordinary (classical) fluid and turbulence in the quantum phases of ^{4}He, ^{3}He and atomic Bose-Einstein condensates. Quantum turbulence[1] shares important features with classical homogeneous isotropic turbulence[2, 3]: the most important is the Kolmogorov $k^{-5/3}$ energy spectrum[4] where k is the wavenumber.

^{4}He consists of two components: an inviscid superfluid components (associated to the quantum ground state) and thermal excitations, which make up a viscous normal fluid component. What makes helium particularly interesting is that superfluid vorticity is concentrated in line singularities of fixed circulation $\kappa = h/m$, where h is Planck's constant and m is the mass of one helium atom (in ^{3}He the relevant boson is a Cooper pair). Normal fluid vorticity is unconstrained, as in classical flows. Turbulence in ^{4}He is thus a complex doubly-turbulent regime, in which a viscous fluid interacts with discrete inviscid vortex lines.

The intensity of quantum turbulence is characterized by the vortex line density L (vortex length per unit volume). In a striking experiment, Roche *et al.*[5] measured the fluctuations of L in turbulent ^{4}He. They observed that the frequency spectrum scales as $f^{-5/3}$, where f is the frequency. The same scaling was observed in turbulent ^{3}He[6]. The rapid decrease of the spectrum is surprising because, if one interprets L as a measure of the rms superfuid vorticity ($\omega_s = \kappa L$), it seems to contradict the classical scaling of vorticity [7] expected from the Kolmogorov energy spectrum, which increases with k. The aim of this letter is to shed light onto this problem.

Since the typical distance between superfluid vortices $\ell \approx L^{-1/2}$ is orders of magnitude bigger than the vortex core radius a_0, we model vortices as space curves $\mathbf{s}(\xi, t)$ where ξ is arclength and t is time. The curves are numerically discretised by a large, variable number of points $\mathbf{s}_j$ $(j = 1, \cdots N)$. The governing equation is [8]

$$\frac{d\mathbf{s}}{dt} = \mathbf{v}_s + \alpha \mathbf{s}' \times (\mathbf{v}_n - \mathbf{v}_s) - \alpha' \mathbf{s}' \times [\mathbf{s}' \times (\mathbf{v}_n - \mathbf{v}_s)] \,, \tag{1}$$

where $\mathbf{s}' = d\mathbf{s}/d\xi$ is the unit tangent vector at $\mathbf{s}$, α, α' are temperature dependent friction coefficients [9], $\mathbf{v}_n$ is the normal fluid's velocity, and the velocity $\mathbf{v}_s$ which the vortex lines induce on each other at the point $\mathbf{s}$ is given by the Biot-Savart (BS) law:

$$\mathbf{v}_s = -\frac{\kappa}{4\pi} \oint_{\mathcal{L}} \frac{(\mathbf{s} - \mathbf{r})}{|\mathbf{s} - \mathbf{r}|^3} \times \mathbf{dr}. \tag{2}$$

The line integral extends over the entire vortex configuration $\mathcal{L}$. Vortex lines reconnect[10] when they become sufficiently close to each other, provided that the total length (as a proxy for energy) is reduced[11]. The discretization technique is standard[12]; the reconnection technique and the de-singularization of the BS integral are described elsewhere[13].

The difficulty of this vortex filament method is the computational cost of the BS law which scales as N^2 (the velocity at one point depends on an integral over all other $N-1$ points); this prevents calculations of intense vortex tangles (large N) for sufficiently long times to make realistic comparison with experiments. The same difficulty arises in astrophysical N-body simulations (the force of gravity on one body depends on the other $N-1$ bodies); in this context, the problem was solved by the development of tree algorithms [14] whose computational cost scale as $N \log(N)$ with small loss of accuracy [15, 16].

To achieve our aim we have developed the following tree algorithm for vortex dynamics. At each time step, points are grouped in a hierarchy of cubes which is arranged in a three-dimensional oct-tree structure. We construct the tree top down, first dividing the computational box (root) into eight cubes, and then continuing to divide each cube into eight 'children', until either a cube is empty or only contains one point. As we create the tree, we calculate the total vorticity contained within each cube and the 'center of vorticity' of the cube from the points that it contains. The time required for constructing the tree scales as $N \log(N)$, so it feasible to 'redraw' the tree at each time step. Fig. 1 illustrates this procedure in two dimensions.

To calculate the induced velocity $\mathbf{v}_s$ at each point $\mathbf{s}$ we must 'walk' the tree, and decide if a cube is sufficiently far. This is done using the concept of the opening angle θ [14] (as corrected by Barnes[16, 17] to avoid errors if the center of vorticity is near the edge of the cube). Let w be the width of the cube, d the distance of the center of vorticity from $\mathbf{s}$ and δ the distance from the center of vorticity and the geometrical center of the cube. If $d > w/\theta + \delta$ we accept the cube, and its contribution is used in computing the velocity via Eq. 2. If not, then we open the cube (assuming it contains more that one point) and repeat the test on each of the child cubes that it contains. The tree-walk ends when the contributions of all cubes have been evaluated.

We tested the tree algorithm up to $N = 2000$ points (practical limit of the BS law) using different values of θ. We verified the $N \log(N)$ scaling for both the construction of the tree and the calculation of the total velocity. We found that the relative deviation of the velocity computed via the tree algorithm from the exact BS velocity is at the most 0.25% if $\theta = 0.7$, which we take as the critical opening angle hereafter.

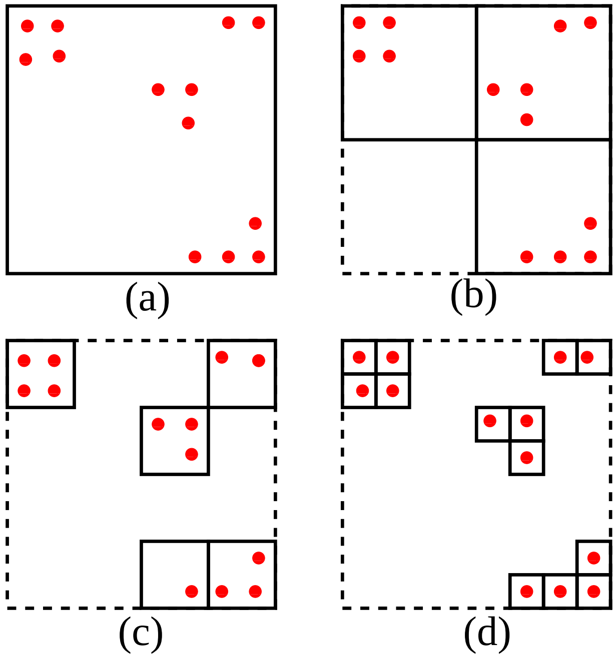

FIG. 1. (Color online) Illustration of the tree construction in two dimensions (quad-tree). The points (red dots) are inclosed in the root cell (a), which is divided into four cells of half size (b), until (c,d) there is only one point per cell.

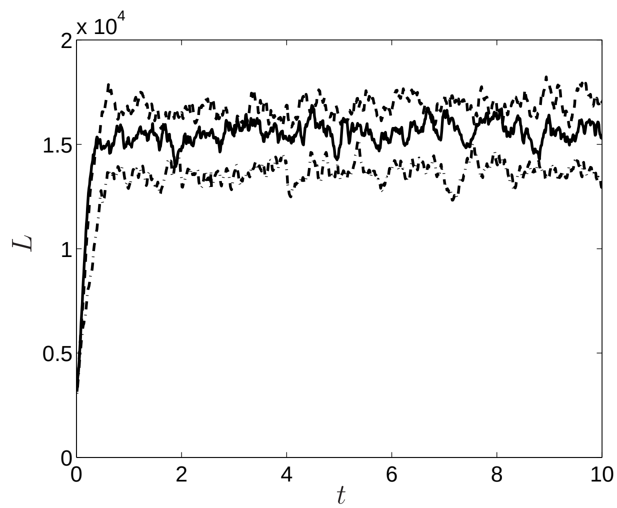

FIG. 2. Vortex line density L (cm^{-2}) vs time t (s) corresponding to $\mathrm{Re}_n = 22.7$ (dot-dashed line), $\mathrm{Re}_n = 57.1$ (solid line), and $\mathrm{Re}_n = 112.9$ (dashed line).

The computational box is a cube of size $D = 0.075$ cm with periodic boundary conditions. When evaluating the BS integral, for each point in the box we consider the other $3^3 - 1 = 26$ boxes around it; this periodic wrapping is easily obtained using the tree structure..

To model the turbulent normal fluid of the experiment[5] we use a Kinematic Simulation (KS) [18], in which the normal fluid velocity at position $\mathbf{s}$ and time t is prescribed by the following sum of M random Fourier modes:

$$\mathbf{v}_n(\mathbf{s}, t) = \sum_{m=1}^{M} \left(\mathbf{A}_m \times \mathbf{k}_m \cos\phi_m + \mathbf{B}_m \times \mathbf{k}_m \sin\phi_m \right), \tag{3}$$

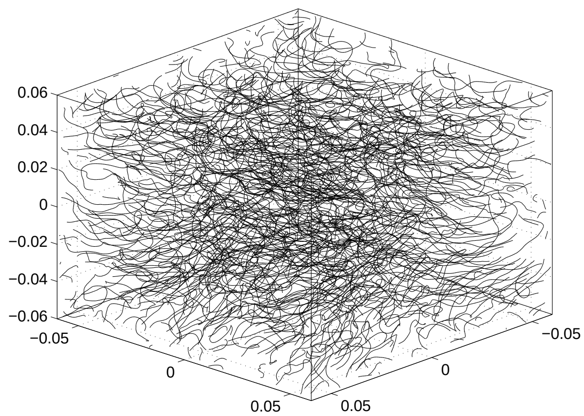

FIG. 3. Saturated vortex tangle at $t = 2.0$ s with $N = 55,359$ and $L = 91,733$ cm^{-2}, corresponding to $\mathrm{Re}_n = 507$.

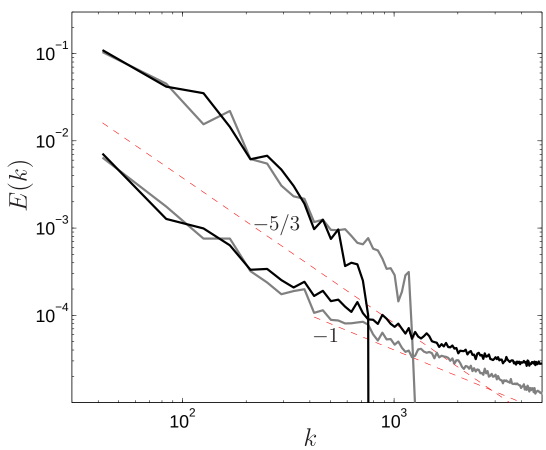

FIG. 4. (Color online). Normal fluid's (upper two lines) and superfluid's (lower two lines) energy spectrum $E(k)$ vs k (cm^{-1}). Grey lines: $\mathrm{Re}_n = 112.9$ ($L = 8889$ cm^{-2}, $k_\ell = 2\pi/\ell = 592$ cm^{-1}); black lines: $Re_\mathrm{n} = 49.85$ ($L = 7058$ cm^{-2}, $k_\ell = 527$ cm^{-1}). Dashed lines: $k^{-5/3}$ (top) and k^{-1} (bottom) scalings.

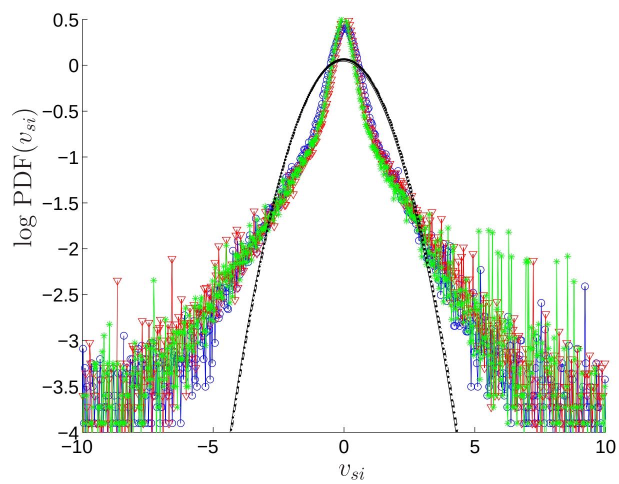

FIG. 5. (Color online) PDF of superfluid velocity components (cm/s) v_{sx} (blue circles), v_{sy} (red triangles) and v_{sz} (green asterisks) sampled over the vortex-points for $\mathrm{Re}_n = 112.9$. The overlapping black dotted, dash dotted and solid lines are respectively the Gaussian fits to the same data, $\mathrm{gPDF}(v_{si}) = (1/(\sigma\sqrt{2\pi}))\exp\left(-(v_{si} - \tilde{\mu})^2/(2\sigma^2)\right)$, $(i = 1, 2, 3)$ where σ and $\tilde{\mu}$ are the standard deviation and the mean.

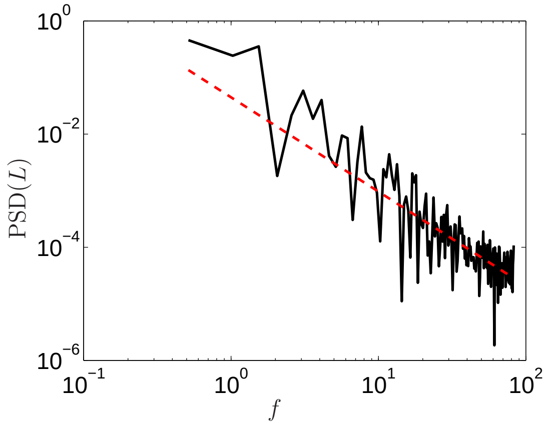

FIG. 6. (Color online). Power spectral density of fluctuations of L (arbitrary units) vs f (s^{-1}) at $t = 10$ s corresponding to $\mathrm{Re}_n = 507$ as in Fig. 3. The best fit to the data is $f^{-1.71}$. The dashed line shows the $f^{-5/3}$ scaling.

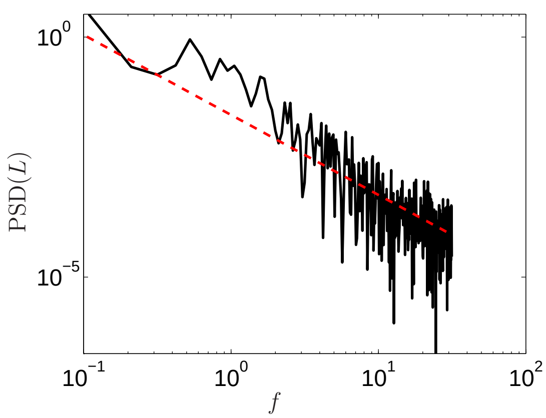

FIG. 7. (Color online). Power spectral density of fluctuations of length of reconnecting material lines (arbitrary units) vs f (s^{-1}) at $t = 10$s, corresponding to $\mathrm{Re}_n = 33.28$. The best fit to the data is $f^{-1.74}$. The dashed line shows the $f^{-5/3}$ scaling.

with $\phi_m = \mathbf{k}_m \cdot \mathbf{s} + \omega_m t$, where $\mathbf{k}_m$ and $\omega_m = \sqrt{k_m^3 E(k_m)}$ are wavevectors and frequencies. Via an appropriate choice of $\mathbf{A}_m$ and $\mathbf{B}_m$, the energy spectrum of $\mathbf{v}_n$ reduces to the Kolmogorov form $E(k_m) \propto k_m^{-5/3}$ for $1 \ll k \ll k_M$, with $k = 1$ at the integral scale and k_M at the cut-off scale. The effective Reynolds number $\mathrm{Re}_n = (k_M/k_1)^{4/3}$ is defined by the condition that the dissipation time equals the eddy turnover time at $k = k_M$. Like some [19] previous implementations of KS, we have adapted Eq. 3 to periodic boundary conditions. In summary, $\mathbf{v}_n$ is solenoidal, time-dependent, and satisfies the main properties of homogeneous isotropic turbulence, from the energy spectrum to two-points statistics.

We use parameters which refer to ^{4}He: circulation $\kappa = 9.97 \times 10^{-4}$ cm^2/s and vortex core radius $a_0 = 10^{-8}$ cm. We choose $T = 2.164$ K ($\alpha = 1.21$ and $\alpha' = -0.3883$), larger than in Ref. [5], in order that the back reaction of the vortex lines on the normal fluid is negligible and Eq. 3 is justified. Our calculation has thus two independent parameters: T and Re_n. The initial condition consists of 16 straight vortices at random positions and orientations.

Figure 2 shows time series of the vortex line density at three different values of Re_n. In each case the initial growth is followed by saturation to a statistical steady state in which L fluctuates around a mean value. An example of a saturated vortex tangle is shown in Fig. 3. By harnessing the power of the tree algorithm we have performed calculations with up to $N = 400,000$ points.

We construct a 512^2 mesh in the $xy-$plane at the center of the box. At each mesh point we calculate $\mathbf{v}_s$ and $\mathbf{v}_n$, using the tree approximation to the BS integral and Eq. 3 respectively. The corresponding energy spectra for two values of Re_n are shown in Fig. 4. The $k^{-5/3}$ Kolmogorov spectrum of the normal fluid is clearly visible. The superfluid follows the Kolmogorov scaling in the inertial range $1 \ll k \ll k_M$, in agreement with experiments[4]. In the range $k > k_M$ the normal fluid is essentially at rest, and the friction dampens Kelvin waves on quantized vortices (preventing a cascade of energy to larger k which would happen if $\alpha = \alpha' = 0$, as discussed in Ref. [13]); a k^{-1} scaling,

typical of individual straight vortex lines, is visible in this range.

Despite the classical nature of the superfluid energy spectrum, the statistics of superfluid velocity components display power-law behavior. The probability density functions (normalized histogram, or PDF for short) scale as $\mathrm{PDF}(v_{s,i}) \propto v_{si}^b$ $(i = 1, 2, 3)$ with average exponent $b = -3.1$, see Fig. 5. This scaling was observed in turbulent helium experiments [20], and was calculated in turbulent atomic condensates[21] and helium counterflow[22]; its cause is the singular nature of the superfluid vorticity[21]. The vortex line velocity $d\mathbf{s}/dt$ obeys non-Gaussian scaling too. The statistics of velocity components in ordinary turbulence, on the contrary, are Gaussian[23].

Finally we compute the frequency spectrum of the fluctuations of the vortex line density in the saturated state. Fig. 6 shows that the spectrum scales as $f^{-5/3}$, for large f, as observed in the experiments [5, 6]. The fact that the high frequency regime where this scaling takes place is not exactly the same as in the experiment is less important, and arises from our choice of temperature, hence the value of saturated L. We observe the same $f^{-5/3}$ scaling at all values of turbulent intensities Re_n.

What is the reason for this scaling ? Roche *et al.* [24, 25] argued that the more randomly oriented vortex lines (which particularly contribute to line length and second sound attenuation) have some of the statistical properties of passive scalars. To test this idea we perform numerical simulations in which vortex filaments are replaced by passive material lines which evolve according to $d\mathbf{s}/dt = \mathbf{v}_n$ (we do not switch off the reconnection algorithm, otherwise the vortex length would grow indefinitevely). We find that the length saturates at values larger than the vortex line density and that the spectrum of the fluctuations scales again as $f^{-5/3}$, as in Fig. 6. Being L positive definite[26], there is no conflict with the vorticity spectrum.

In conclusion, our calculations reproduce the main observed features of quantum turbulence: (i) the classical $k^{-5/3}$ scaling of the energy spectrum observed at large scales by Tabeling[4] (thought to be associated with large-scale, energy-containing polarization of vortex lines[2]); (ii) the observation of non classical (non Gaussian) velocity statistics[20] (macroscopic manifestation of singular vorticity[21]); and (iii) the $f^{-5/3}$ spectrum of the vortex line density fluctuations observed at large frequency[5, 6]. The natural question is whether they are independent. Our results also support Roche's interpretation[24] that vortex density fluctuations arise from random vortex lines which behave as reconnecting material lines (while most of the tangle's energy is in the large scale motion).

The vortex tree algorithm could be further speeded up by parallelization[27]. Its power should allow us to tackle problems which require large N, for example the detection of anomalous scaling[28] and, in the $T = 0$ limit, the transition from the Kolmogorov energy cascade at small k to the Kelvin waves cascade at big k [29].

---

[1] S.K. Nemirovskii, W. Fiszdon Rev. Mod. Phys. **67**, 37 (1995).

[2] W.F. Vinen and J.J. Niemela, J. Low Temp. Phys. **128**, 167 (2002),

[3] L. Skrbek, J. Low Temp. Phys. **161**, 555 (2010).

[4] J. Maurer and P. Tabeling, Europhys. Lett. **43**, 29 (1998);

[5] P.-E. Roche, P. Diribarne, T. Didelot, O. Français, L. Rousseau, and H. Willaime, Europhys. Lett. **77**, 66002 (2007).

[6] D. I. Bradley, S. N. Fisher, A. M. Guénault, R. P. Haley, S. O'Sullivan, G. R. Pickett, and V. Tsepelin, Phys. Rev. Lett. **101**, 065302 (2008);

[7] M. Farge, K. Schneider, G. Pellegrino, A.A. Wray and R.S. Rogallo, Phys. of Fluids **15**, 2886 (2003).

[8] K.W. Schwarz, Phys. Rev. B **38**, 2398 (1988).

[9] C.F. Barenghi, R.J. Donnelly and W.F. Vinen, J. Low Temp. Phys. **52**, 189 (1983); R.J. Donnelly, and C.F. Barenghi, J. Phys. Chem. Ref. Data **27**, 1217 (1998).

[10] G.P. Bewley, M.S. Paoletti, K.R. Sreenivasan, and D.P. Lathrop, P.N.A.S. **105**, 13707 (2008); R. Tebbs, A.J. Youd and C.F. Barenghi, J. Low Temp. Physics **162**, 314 (2011); R.M. Kerr, arXiv:1006.3911v2, 21 Sept 2010; M. Kursa, K. Bajer, and T. Lipniacki, Phys. Rev. B **83**, 014515 (2011).

[11] M. Leadbeater, T. Winiecki, D.C. Samuels, C.F Barenghi, and C.S. Adams, Phys. Rev. Lett. **86**, 1410 (2001).

[12] During the evolution new points are introduced (using quadratic interpolation) if the distance between two neighboring points along a vortex becomes larger than $\Delta\xi_{min} = 0.001$ cm. Similarly points are removed, keeping their mutual distance comprised between $\Delta\xi_{min}$ and $\Delta\xi_{min}/2$. Time evolution is based on a 3^{rd} order Adams-Bashforth scheme (the time step Δt depends on $\Delta\xi_{min}$ to resolve the shortest Kelvin waves).

[13] A.W. Baggaley and C.F. Barenghi, Phys. Rev. B **83**, 134509 (2011).

[14] J. Barnes, and P. Hut, Nature **324**, 446 (1986).

[15] E. Bertschinger, Ann. Review Astronomy and Astrophysics **36**, 599 (1998).

[16] J. Barnes, in *Computational Astrophysics* ed. by J. Barnes et al., Springer-Verlag, Berlin (1994).

[17] J. Dubinski, New Astronomy **1**, 133 (1996)

[18] D.R. Osborne, J.C. Vassilicos, K. Sung, and J.D. Haigh, Phys. Rev. E, **74**, 036309 (2006).

[19] S.L. Wilkin, C.F. Barenghi and A. Shukurov, Phys. Rev. Lett. **99**, 134501 (2007)

[20] M.S. Paoletti, M.E. Fisher, K.R. Sreenivasan, and D.P. Lathrop, Phys. Rev. Lett. **101**, 154501 (2008).

[21] A.C. White, C.F. Barenghi, N.P. Proukakis, A.J. Youd, and D.H. Wacks, Phys. Rev. Lett., **104**, 075301 (2010).

[22] H. Adachi and M. Tsubota, Phys. Rev. B **83**, 132503 (2011).
[23] A. Vincent and M. Meneguzzi, J. Fluid Mech. **225**, 1 (1991); A. Noullez *et al.* , J. Fluid Mech. **339**, 287 (1997); T. Gotoh *et al.* , Phys. of Fluids **14**, 1065 (2002).
[24] P.-E. Roche and C.F. Barenghi, Europhys. Lett. **81**, 36002 (2008).
[25] J. Salort, P.-E. Roche, and E. Leveque, (to be published)
[26] T. Ishihara, Y. Kaneda, M. Yokokawa, K. Itakura. and A. Uno, J. Phys. Soc. Japan **72**, 983 (2003).
[27] V. Springel *et al.* Nature **435**, 629 (2005).
[28] U. Frisch, *Turbulence: the legacy of A.N. Kolmogorov*, Cambridge U. Press (1995).
[29] V.S. L'vov, S.V. Nazarenko and O. Rudenko, Phys. Rev. B **76**, 024520 (2007); E. Kozik and B. Svistunov, Phys. Rev. B **77**, 060502 (2008).